RAPID COMMUNICATIONS IN MASS SPECTROMETRY
Rapid Commun. Mass Spectrom. 2006; **20**: 157–170
Published online in Wiley InterScience (www.interscience.wiley.com). DOI: 10.1002/rcm.2283

RCM

Differentiation of three pairs of aconite alkaloid isomers from *Aconitum nagarum* var. *lasiandrum* by electrospray ionization tandem mass spectrometry

Rui Li, Zhijun Wu, Fan Zhang and Lisheng Ding*
Chengdu Institute of Biology, Chinese Academy of Sciences, Chengdu 610041, PR China

Received 18 August 2005; Revised 31 October 2005; Accepted 7 November 2005

Three pairs of isomers of aconite alkaloids from *Aconitum nagarum* var. *lasiandrum* have been investigated by electrospray ionization mass spectrometry (ESI-MS) and tandem mass spectrometry (MS/MS) employing ion-trap and quadrupole time-of-flight mass spectrometers in positive mode. Based on the differences of their fragmentation pathways and special fragment ions, three pairs of isomers of aconite alkaloids were differentiated. In addition, fragmentation laws of some veatchines and the discrepancy of fragmentation mechanisms between veatchine-type and aconitine-type alkaloid were also concluded. In the case of veatchines, a radical would be formed by homolysis of C18–C4 or C18–H bonds, followed by elimination of a series of C_2H_2 and C_2H_4. Moreover, the retro-Diels-Alder (RDA) reaction occurred in the E-ring and double-electron transfer triggered by the positive charge on C1 led to the formation of diagnostic ions at *m/z* 216. With regard to aconitine-type alkaloids, the N-substituent is not eliminated easily. Although there is no carbonyl group on some aconitine-type alkaloids, with hydroxyl and methoxyl on C15 and C16 respectively, CO was readily eliminated through tautomerization. Copyright © 2005 John Wiley & Sons, Ltd.

Aconitum nagarum var. *lasiandrum* (Ranuculaceae) is mainly distributed in the Yunnan Province of China. Its roots can relieve pain and dispel dampness. The roots of this species have been used as a folk medicine in China for the treatment of cold limbs in syncope, epigastric pain, vomiting and diarrhea.[1] The chemical constituents of this plant have been investigated,[1,2] and it is rich in aconite alkaloids that can be divided into four groups according to the structure of their skeleton: atisine, veatchine, aconitine and lycoctonine types. For pharmacologically and structurally interesting substances from traditional Chinese medicines, we investigated the chemical compounds of *Aconitum nagarum* var. *lasiandrum* to afford 21 compounds, among which there are three pairs of isomers: compounds A1 and A2 (MW 359 Da); compounds B1 and B2 (MW 357 Da); and compounds C1 and C2 (MW 629 Da). Their possible molecular structures according to the literature are depicted in Table 1.

Mass spectrometry (MS) provides a complementary method for high sensitivity, selectivity and speed of analysis. Up till now, studies on the characterization of isolated alkaloids,[3–6] the quantification and stereochemistry of aconite alkaloids[7–10] have been performed by various MS techniques. Electrospray ionization (ESI) with an ion-trap (IT) analyzer is a powerful tool in characterizing the fragmentation mechanism, which can provide some genealogy of ion formation by multi-stage tandem mass spectrometry. ESI with a quadrupole time-of-flight (Qq-TOF) analyzer is an effective analytical method, which combines the exact mass information about the quasi-molecular ion obtained from the first-order mass spectrum and additional structural information based on tandem mass spectrometric (MS/MS) analyses that can bombard the precursor ions into small fragment ions. Thus we can acquire much information about the sample ions and presume their structures; hence some isomers can also be differentiated Table 2.

Liu and coworkers have carried out many studies on the aconitine-type alkaloids by ESI-MS/MS.[11,12] Fragmentation pathways of aconitine-type alkaloids were concluded as the elimination of peripheral acid or fatty acid moieties and successive losses of 1–4 CH_3OH molecules, 1–3 H_2O and CO. By applying knowledge of these fragmentation pathways to the aconitine-type alkaloids in the ethanolic extract of aconite roots, all the 16 known aconitine-type alkaloids were detected. To our knowledge, little attention was paid to the determination of the fragmentation mechanism of veatchines and utilization of the laws in differentiation of isomers of aconite alkaloids using ESI-QqTOF-MS and ESI-IT-MS^n. In this work, three pairs of isomers of aconite alkaloids from the roots of *Aconitum nagarum* were distinguished by ESI-IT-MS^n and ESI-QqTOF-MS/MS techniques and the fragmentation mechanisms were also suggested.

EXPERIMENTAL

Chemicals and solutions

Unless specified otherwise, all chemicals and solvents were of analytical reagent grade and were obtained from Chengdu

*Correspondence to: L. Ding, Chengdu Institute of Biology, Chinese Academy of Sciences, Chengdu 610041, PR China.
E-mail: lsding@cib.ac.cn

RCM

Table 1. The possible molecular structures of the three pairs of isomers

Isomers	MW	Possible molecular structures
A1 and A2	359 Da	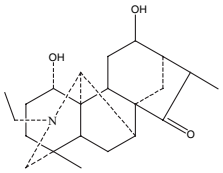 karakomine 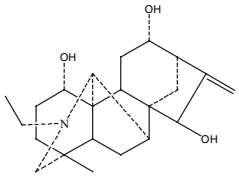 napelline
B1 and B2	357 Da	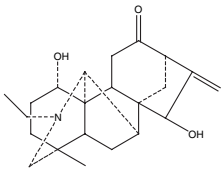 songorine 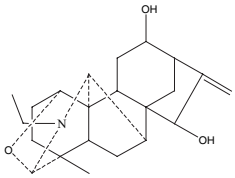 12-*epi*-dehydronapelline
C1 and C2	629 Da	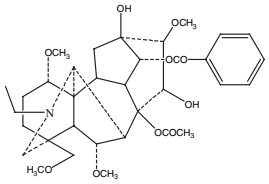 deoxyaconitine 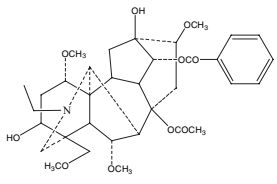 indaconitine

Table 2. Accurate mass measurements and elemental compositions of isomers and some product ions using ESI-QqTOF-MS/MS analysis

Compound	Measured mass ($[M+H]^+$)	Major ions	CE (eV)	Caculated mass	Elemental composition	Error (ppm)
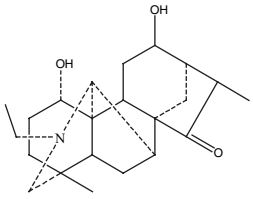 karakomine A1	360.2520	360.2525	30	360.2522	$C_{22}H_{34}NO_3^+$	0.83
		342.2427	30	342.2422	$C_{22}H_{32}NO_2^+$	1.46
		324.2330	30	324.2322	$C_{22}H_{30}NO^+$	2.47
		314.2128	30	314.2109	$C_{20}H_{28}NO_2^+$	6.05
		314.2462	30	314.2484	$C_{21}H_{32}NO^+$	−7.00
		300.1951	30	300.1964	$C_{19}H_{26}NO_2^+$	−4.33
		296.2021	30	296.2003	$C_{20}H_{26}NO^+$	6.08
		296.2357	30	296.2378	$C_{21}H_{30}N^+$	−7.09
		295.1917	30	295.1931	$C_{20}H_{25}NO^{\cdot+}$	−4.74
		268.2060	30	268.2065	$C_{19}H_{26}N^+$	−1.86
		216.1388	30	216.1357	$C_{14}H_{18}NO^+$	14.34
		211.1010	30	211.0992	$C_{14}H_{13}NO^{\cdot+}$	8.53
		190.1246	30	190.1232	$C_{12}H_{16}NO^+$	7.36
		183.0710	30	183.0680	$C_{12}H_9NO^{\cdot+}$	16.39
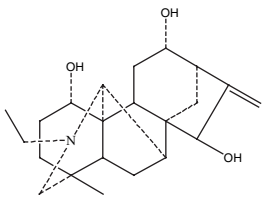 napelline A2	360.2517	360.2516	30	360.2522	$C_{22}H_{34}NO_3^+$	−1.67
		342.2424	30	342.2422	$C_{22}H_{32}NO_2^+$	0.58
		324.2331	30	324.2322	$C_{22}H_{30}NO^+$	2.78
		314.2129	30	314.2109	$C_{20}H_{28}NO_2^+$	6.37
		306.2211	30	306.2216	$C_{22}H_{28}N^+$	−1.63
		296.1997	30	296.2003	$C_{20}H_{26}NO^+$	−2.03
		295.1941	30	295.1931	$C_{20}H_{25}NO^{\cdot+}$	3.39
		281.1754	30	281.1774	$C_{19}H_{23}NO^{\cdot+}$	−7.11
		267.1602	30	267.1618	$C_{18}H_{21}NO^{\cdot+}$	−5.99
		225.1157	30	225.1148	$C_{15}H_{15}NO^{\cdot+}$	4.00
		216.1374	30	216.1383	$C_{14}H_{18}NO^+$	−4.16
		190.1243	30	190.1232	$C_{12}H_{16}NO^+$	5.79

Continues

Table 2. *Continued*

Compound	Measured mass ([M+H]$^+$)	Major ions	CE (eV)	Caculated mass	Elemental composition	Error (ppm)
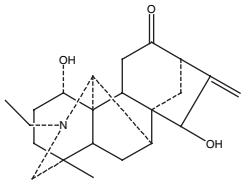 songorine B1	358.2368	358.2366	30	358.2371	$C_{22}H_{32}NO_3^+$	−1.40
		340.2275	30	340.2271	$C_{22}H_{30}NO_2^+$	1.18
		322.2177	30	322.2165	$C_{22}H_{28}NO^+$	3.72
		312.1933	30	312.1964	$C_{20}H_{26}NO_2^+$	−9.93
		312.2311	30	312.2327	$C_{21}H_{30}NO^+$	−5.12
		294.1820	30	294.1852	$C_{20}H_{24}NO^+$	−10.87
		294.2241	30	294.2222	$C_{21}H_{28}N^+$	6.46
		293.1789	30	293.1774	$C_{20}H_{23}NO^{\cdot+}$	5.12
		214.1255	30	214.1232	$C_{14}H_{16}NO^+$	10.74
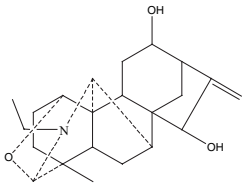 12-*epi*-dehydronapelline B2	358.2363	358.2379	30	358.2377	$C_{22}H_{32}NO_3^+$	0.56
		340.2268	30	340.2271	$C_{22}H_{30}NO_2^+$	−0.88
		322.2171	30	322.2165	$C_{22}H_{28}NO^+$	1.86
		314.2107	30	314.2115	$C_{20}H_{28}NO_2^+$	−2.55
		312.1974	30	312.1958	$C_{20}H_{26}NO_2^+$	5.12
		297.1880	30	297.1852	$C_{20}H_{25}O_2^+$	9.42
		296.1987	30	296.2009	$C_{20}H_{26}NO^+$	−7.43
		294.1831	30	294.1852	$C_{20}H_{24}NO^+$	−7.14
		293.1750	30	293.1774	$C_{20}H_{23}NO^{\cdot+}$	−8.19
		285.1845	30	285.1838	$C_{19}H_{25}O_2^+$	2.45
		279.1703	30	279.1718	$C_{19}H_{21}NO^{\cdot+}$	−5.37
		267.1771	30	267.1743	$C_{19}H_{23}O^+$	10.48
		255.1708	30	255.1732	$C_{18}H_{23}O^+$	−9.41
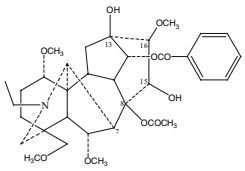 deoxyaconitine C1	630.3270	630.3284	20	630.3273	$C_{34}H_{48}NO_{10}^+$	1.75
		598.3022	20	598.3005	$C_{33}H_{44}NO_9^+$	2.84
		570.3089	20	570.3061	$C_{32}H_{44}NO_8^+$	4.91
		538.2760	20	538.2799	$C_{31}H_{40}NO_7^+$	−7.25
		510.2822	20	510.2850	$C_{30}H_{40}NO_6^+$	−5.49
		506.2501	20	506.2537	$C_{30}H_{36}NO_6^+$	−7.11
		478.2565	20	478.2588	$C_{29}H_{36}NO_5^+$	−4.81
		474.2307	20	474.2275	$C_{29}H_{32}NO_5^+$	6.75
		446.2360	20	446.2326	$C_{28}H_{32}NO_4^+$	7.62
		352.1865	20	352.1907	$C_{22}H_{26}NO_3^+$	−11.93
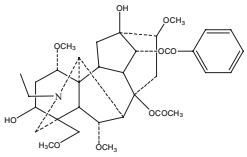 indaconitine C2	630.3261	630.3261	20	630.3237	$C_{34}H_{48}NO_{10}^+$	3.81
		598.2991	20	598.3005	$C_{33}H_{44}NO_9^+$	−2.34
		570.3088	20	570.3061	$C_{32}H_{44}NO_8^+$	4.73
		538.2830	20	538.2799	$C_{31}H_{40}NO_7^+$	5.76
		552.2922	20	552.2956	$C_{32}H_{42}NO_7^+$	−6.16
		520.2652	20	520.2694	$C_{31}H_{38}NO_6^+$	−8.07
		506.2579	20	506.2537	$C_{30}H_{36}NO_6^+$	8.30
		488.2402	20	488.2431	$C_{30}H_{34}NO_5^+$	−5.94
		456.2111	20	456.2169	$C_{29}H_{30}NO_4^+$	−12.71
		334.1845	20	334.1802	$C_{22}H_{24}NO_2^+$	12.87

Chemical Factory (Chengdu, China). Water was purified using a Milli-Q system. The roots of *Aconitum nagarum* var. *lasiandrum* were purchased from a drug store.

Analytical conditions

ESI-MS^n spectra were acquired using a Finnigan LCQ^{DECA} ion-trap mass spectrometer (San Jose, CA, USA) equipped with an ESI source and capable of analyzing ions up to *m/z* 2000. The samples were introduced via a syringe pump at a flow rate of 10 μL/min and spray voltage was set to −5.0 kV in positive mode. The capillary voltage was fixed at 4.0 V and the temperature at 350°C. The ion gauge pressure was 2.4×10^{-5} Torr. Nitrogen was used as a sheath gas at a pressure of 100 psi and the flow rate was 40 arbitrary units. Helium was used as the buffer gas. The ESI interface and mass spectrometer parameters were optimized to obtain maximum sensitivity. For tandem mass spectrometry, the maximum ion injection time was set to 500 ms; the ion isolation width was set at 2.0 Th and the collision energies ranged from 30–40%. The mass scale was calibrated in the positive-ion mode using a solution consisting of caffeine, the tetra-peptide MRFA, and Ultramark 1621 dissolved in a solvent of approximately 25% water, 25% methanol and 50% acetonitrile, acidified to 1% with glacial acetic acid.

High-resolution (HR)-ESI-MS/MS experiments were performed on Bruker BioTOF-Q time-of-flight mass spectrometer equipped with an ESI source (Billerica, MA, USA) in positive-ion mode. High-purity nitrogen gas was used as collision, nebulizer and auxiliary heated gas. The ESI interface conditions were as follows: spray voltage, +6000 V; declustering potential, +40 V; focusing potential, +120 V; neblizer gas flow, 1.5 L/min; auxiliary gas flow 3 L/min; temperature, 400°C. Samples were introduced via a syringe pump at a flow rate of 8 μL/min. The collision energy was set at 20–30 eV and mass data were processed by DataAnalysis 3.2.

RCM

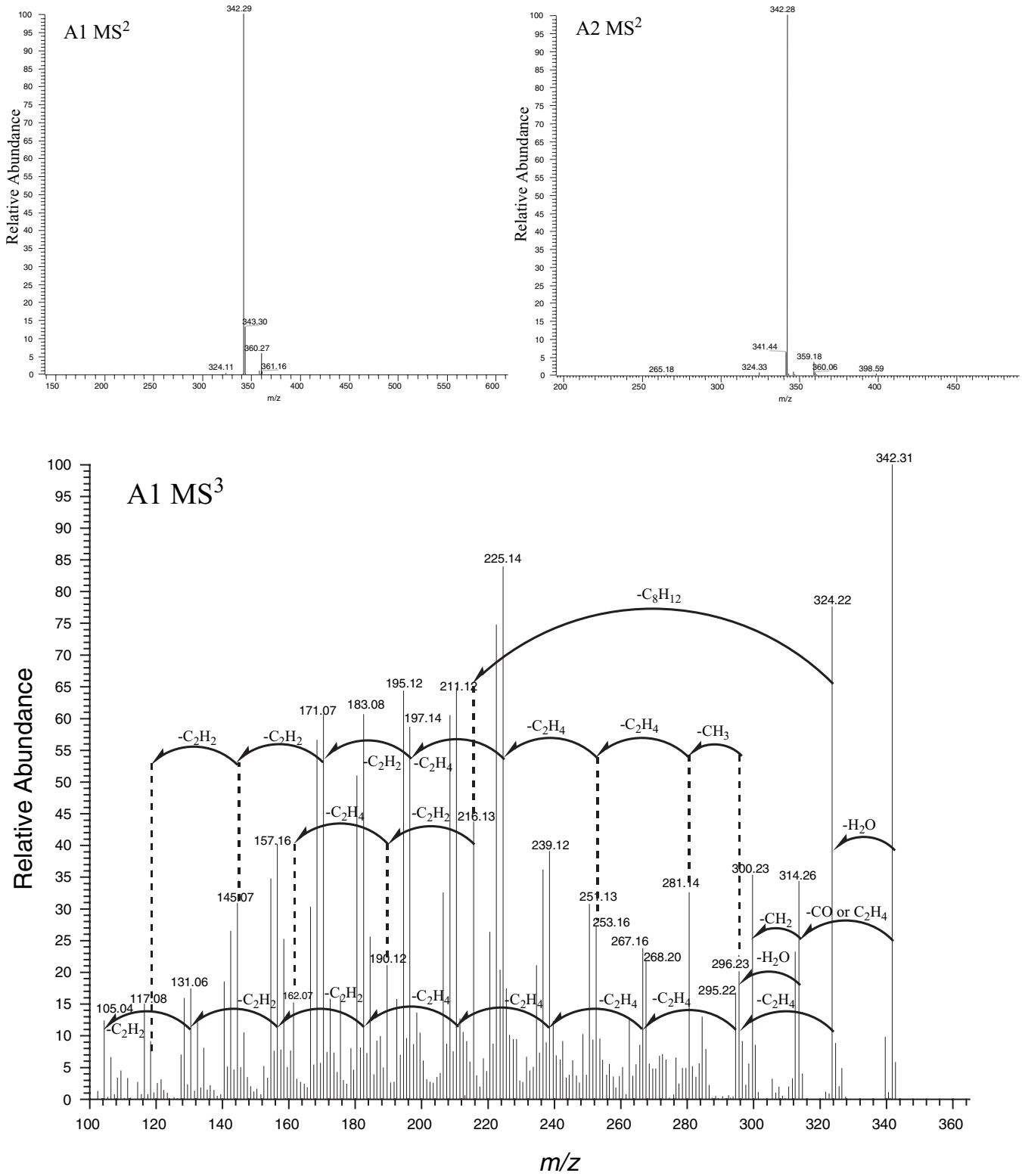

Figure 1. ESI-IT-MS^n mass spectra of isomers A1 and A2. Ions at *m/z* 360 and 342 are the precursor ions in MS^2 and MS^3, respectively.

Preparation of aconite alkaloid sample

Air-dried and powdered roots of *A. nagarum* var. *lasiandrum* (20 kg) were percolated with 70% EtOH at pH 2. The solvent was evaporated *in vacuo* to give approx. 8 kg of an oily mass that was dissolved in 2% HCl. The aqueous phase was extracted with EtOAc. The remaining aqueous phase was progressively basified with NH_4OH to pH 10 to afford a deposit (400 g). This was then extracted with EtOAc to afford the crude alkaloids (150 g). The crude alkaloids were chromatographed over silica gel (160–200 mesh, 1.4 kg) eluted with solvent of increasing polarity [petroleum ether/acetone/diethylamine (12:1:0.1, 10:1:0.1, 8:1:0.1, 6:1:0.1, 4:1:0.1 and

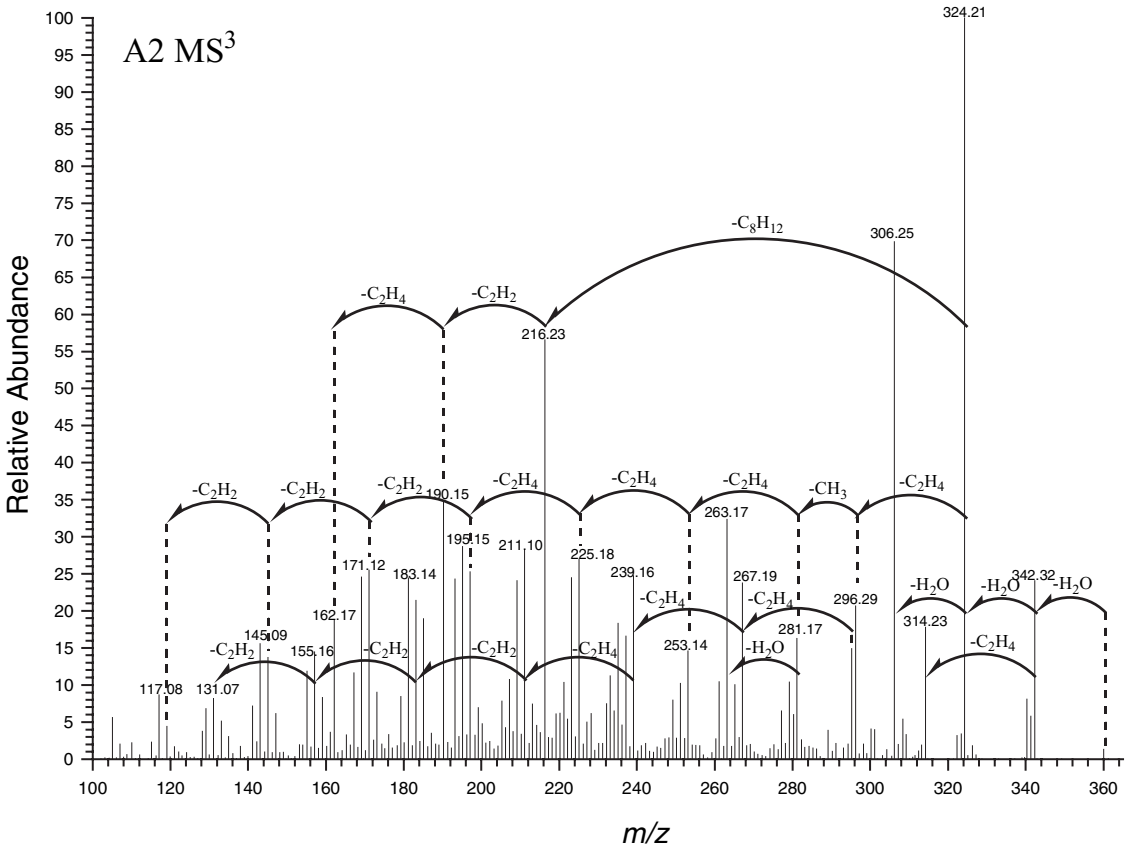

Figure 1. Continued.

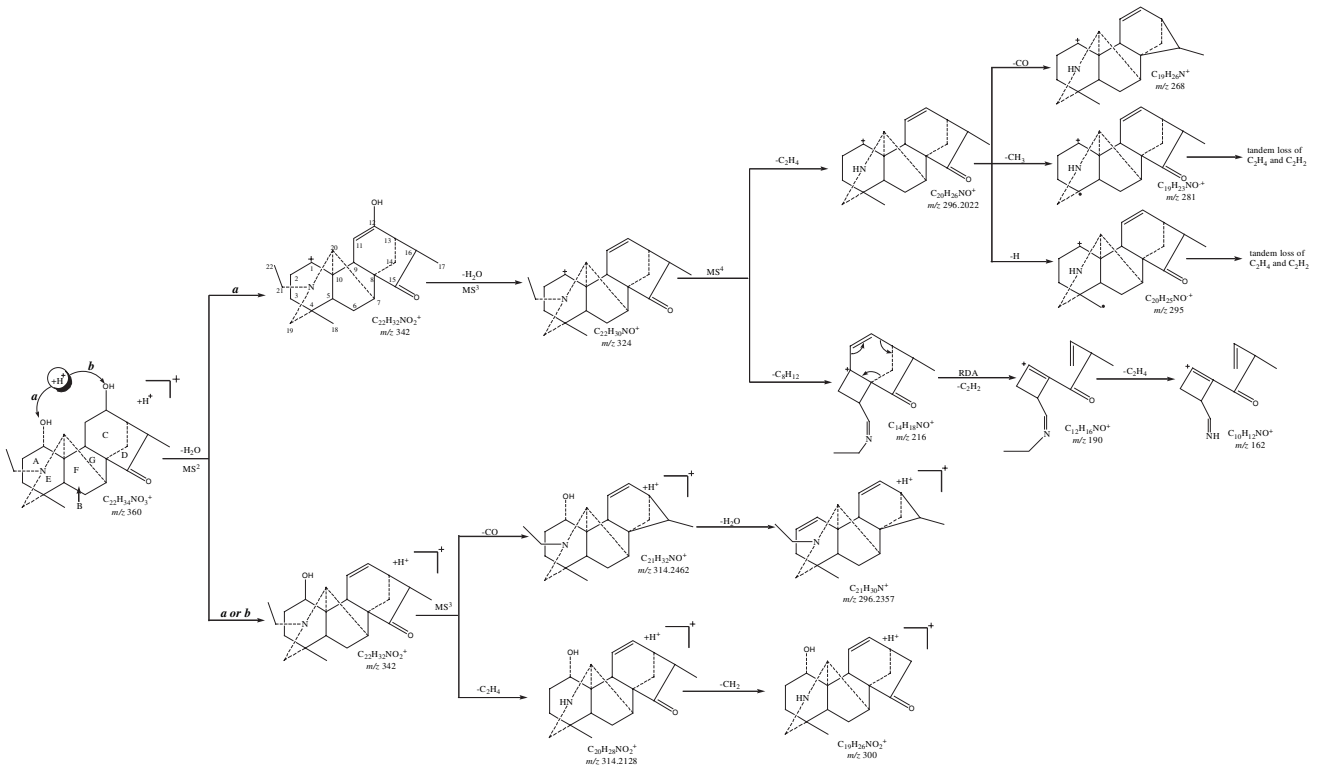

Scheme 1. Proposed fragmentation pathway of karakomine from (+)-ESI-IT-MS^n analysis. Accurate mass measurements of ions acquired by ESI-QqTOF-MS/MS are reported in Table 2.

1:1:0.1), each 5000 mL] to afford frs.1–16 according to analysis by thin-layer chromatography (TLC). Fr.8 (0.8 g) was applied to an ODS silica gel column with MeOH/H_2O (1:3) to give compound A1, Fr.12 (0.9 g) was applied to an ODS silica gel column with MeOH/H_2O (1:3) to give compound A2 (70 mg). Fr.6 (15 g) and fr.7 (5 g) were recrystallized, respectively, with $CHCl_3$ to give compound B1 (10.6 g). Fr.13 (0.06 g) was separated by a neutral aluminum oxide column using petroleum

RCM

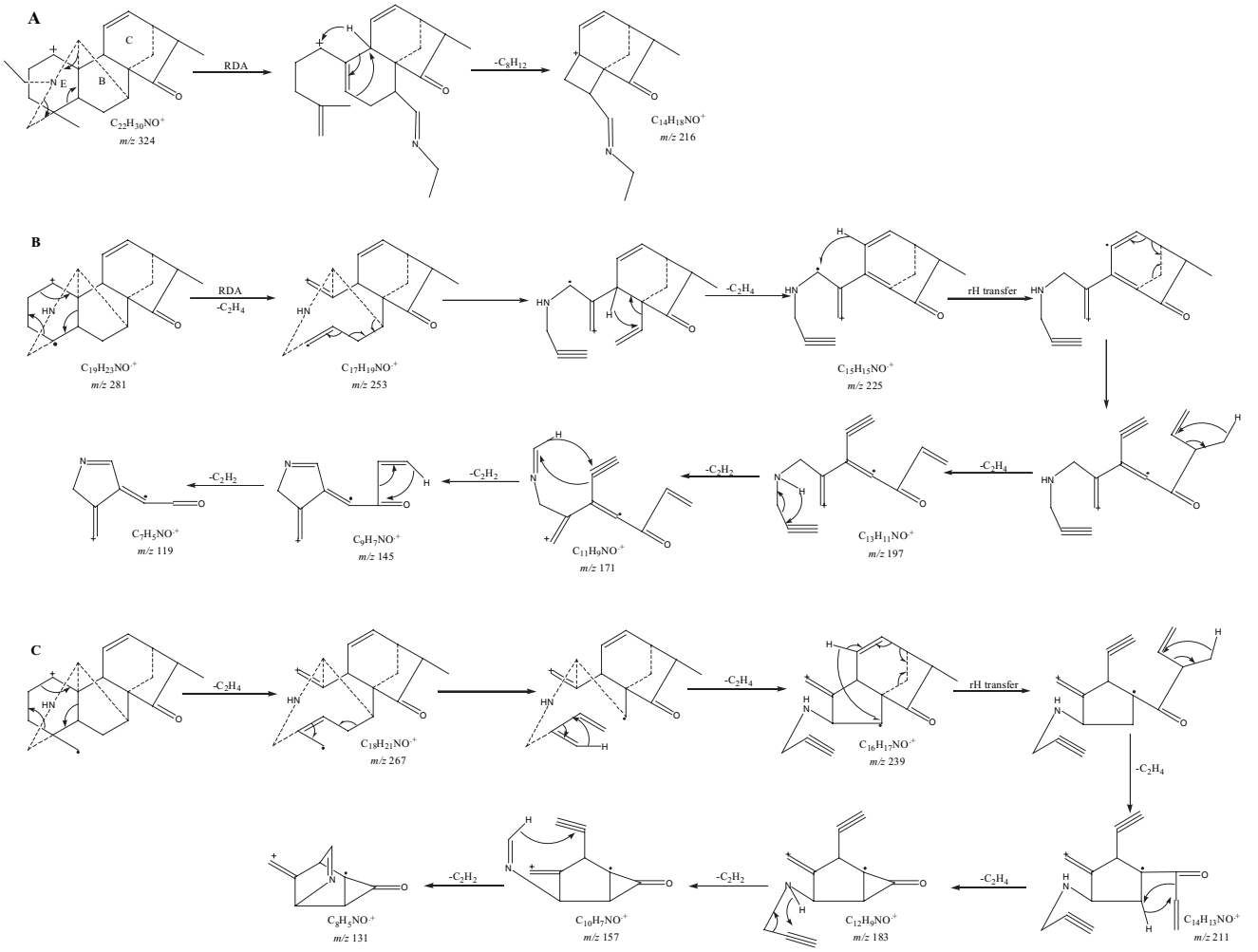

Scheme 2. Mechanisms proposed for fragmentations observed under (+)-ESI-IT-MS^3 analysis: (A) *m/z* 324 → 216; (B) tandem loss of C_2H_4 and C_2H_2 from *m/z* 281; and (C) tandem loss of C_2H_4 and C_2H_2 from *m/z* 295.

ether/acetone (10:1) to give compound B2 (20 mg). Compound C1 (550 mg) was obtained from fr.1 (0.8 g) and fr.2 (0.5 g) by recrystallization with $CHCl_3$. The deposit portion mentioned above was chromatographed over silica gel (160–200 mesh, 1 kg) eluted with a solvent of increasing polarity [petroleum ether/acetone/diethylamine (15:1:0.1, 10:1:0.1, 8:1:0.1, 6:1:0.1, 4:1:0.1 and 1:1:0.1), each 3000 mL] to afford frs.17–21. Fr.18 (0.07 g) was further purified by an ODS silica gel column eluted with MeOH/H_2O (1:3) to give compound C2.

RESULTS AND DISCUSSION

ESI-IT-MS^n and ESI-QqTOF-MS/MS analysis of isomers A1 and A2 (MW 359 Da)

In the positive-ion mode using ESI-IT-MS, both isomers A1 and A2 yielded protonated molecular ions at *m/z* 360, which corresponded to karakomine[13] or napelline[14] according to the literature. There are two hydroxyls and one carbonyl in the peripheral of the karakomine. According to the relative fragmentation mechanisms of alkaloids, two hydroxyls would be lost as two H_2O, while carbonyl would be eliminated as a CO. Napelline has three hydroxyls, which would be eliminated as three H_2O in MS/MS mode. So we can distinguish them using the above differences in the following MS/MS experiments. Fragmentation of the precursor ion (protonated isomers A1 and A2 at *m/z* 360) occurred with a collision energy of 30% to both yield an ion at *m/z* 342, attributable to the loss of H_2O from the precursor ion in the MS^2 experiment (Fig. 1). In the MS^3 experiment of A1 with collision energy of 40%, the fragment ions at *m/z* 324 and 314 were detected, derived from loss of H_2O and CO from the precursor ion at *m/z* 342, respectively. Without the signal of *m/z* 306 corresponding to loss of three H_2O from the precursor ion, isomer A1 might correspond to karakomine. Whereas, in the MS^3 spectrum of isomer A2, the diagnostic fragment ion at *m/z* 306 was observed, indicating that isomer A2 corresponded to napelline. In addition, signals at *m/z* 314 were also detected, which could be explained by loss of an ethylene from the N-substituent. Due to the limitation of the IT analyzer, CO and C_2H_4 cannot be discerned. So, the ion at *m/z* 314 should not be viewed as the diagnostic ion in low-resolution MS. To further validate our assumption, an NMR experiment was also performed and the data were in agreement with our speculation.

In order to further study the fragmentation patterns of veatchine-type alkaloids, HR-ESI-MS/MS was performed and the accurate masses of some fragment ions were

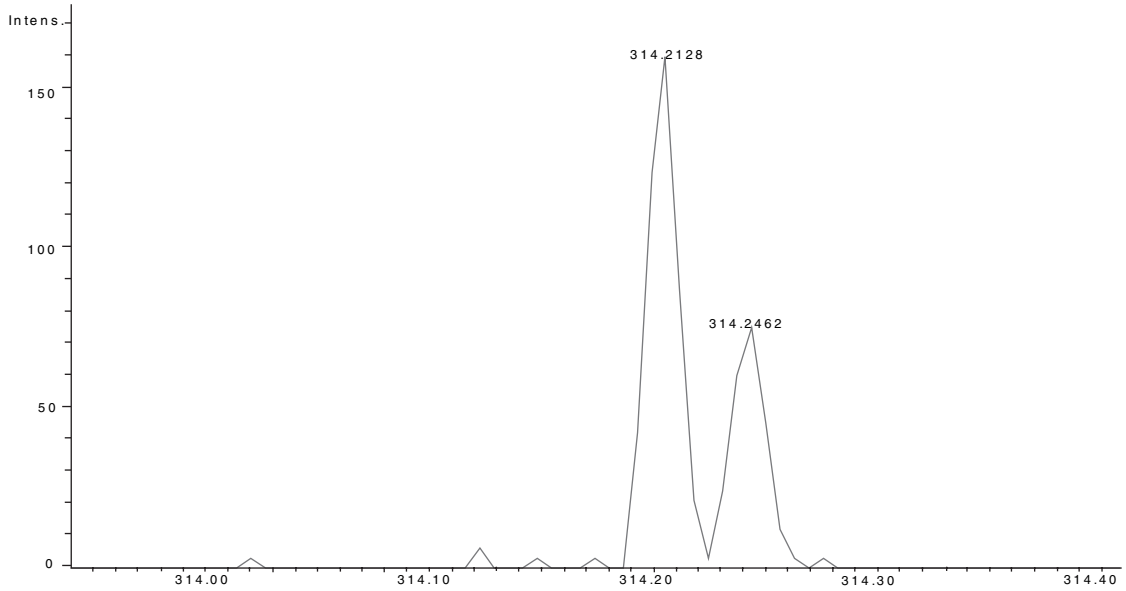

Figure 2. The double peaks at *m/z* 314 observed in ESI-QqTOF-MS/MS of karakomine.

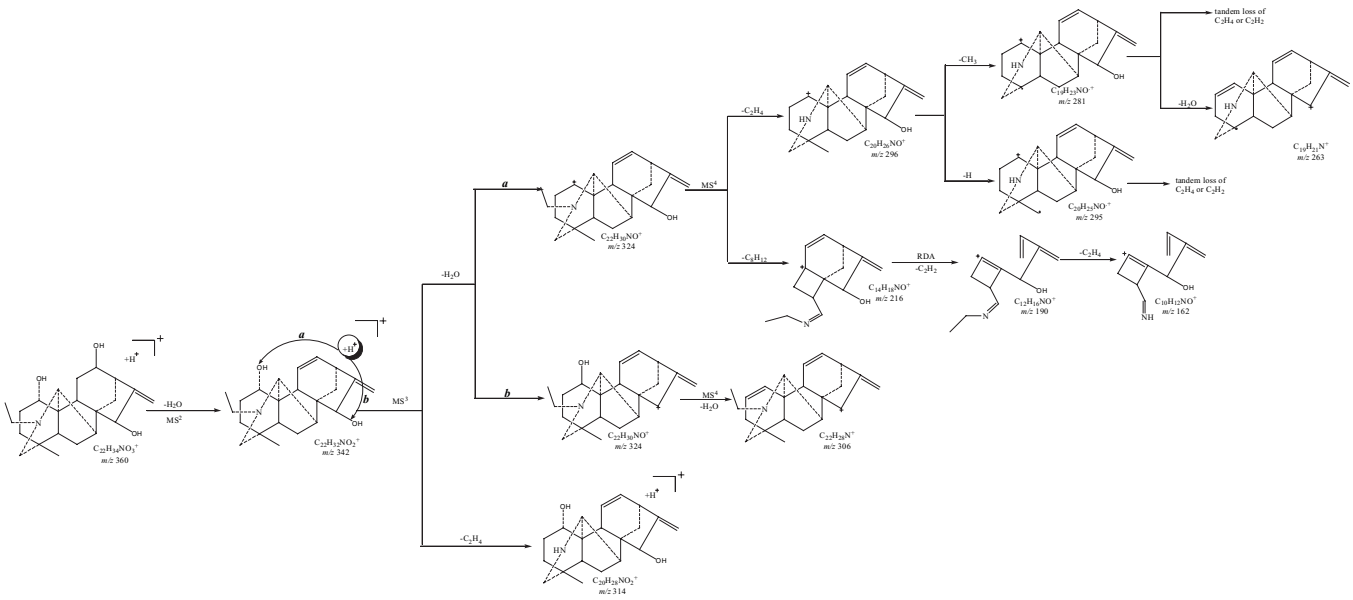

Scheme 3. Proposed fragmentation pathway of napelline from (+)-ESI-IT-MS^n analysis. Accurate mass measurements of ions acquired on ESI-QqTOF-MS/MS are reported in Table 2.

obtained, by which the fragmentation mechanisms of karakomine and napelline were proposed. Scheme 1 shows the fragmentation pattern of karakomine (A1). In an MS^3 experiment of karakomine with collision energy of 40%, the ion at *m/z* 342 (the precursor ion) dissociated to produce a complex fragmentation pattern. The ion at *m/z* 324 was formed by the loss of H_2O from the precursor ion, which fragmented further to generate the ions at *m/z* 296 and 216. The ion at *m/z* 296 could be attributed to the loss of the N-substituent as a molecule of ethylene. Then it was followed by loss of CO from C8 to produce the ion at *m/z* 268. The ions at *m/z* 281 and 295 were produced by the elimination of the CH_3 radical and hydrogen from the ion at *m/z* 296 via the homolysis of C4–C18 and C18–H bonds, respectively. The ion at *m/z* 216, located in a series of odd-mass fragment ions, was conspicuous, which could be explained by a retro-Diels-Alder (RDA) reaction of the E-ring followed by a series of double-electron transfers triggered by the positive charge on C1 (Scheme 2(A)). Then, the ion at *m/z* 216 fragmented with the initial loss of C_2H_2 via the RDA reaction of the C-ring (*m/z* 190), followed by loss of an ethylene from the N-substituent to generate a peak at *m/z* 162. It must be pointed out that the signal at *m/z* 314 acquired by ESI-IT-MS^n corresponded to the double peaks at *m/z* 314.2462 and 314.2128 observed in ESI-TOF-MS/MS (Fig. 2), which could be attributed to loss of CO and C_2H_4 from the precursor ion, respectively. However, without a carbonyl in napelline, only the ethylene could be eliminated to produce the single peak at *m/z* 314.2129. Thus, using HRMS, karakomine and napelline can also be distinguished through the peak number at *m/z* 314. Next,

RCM

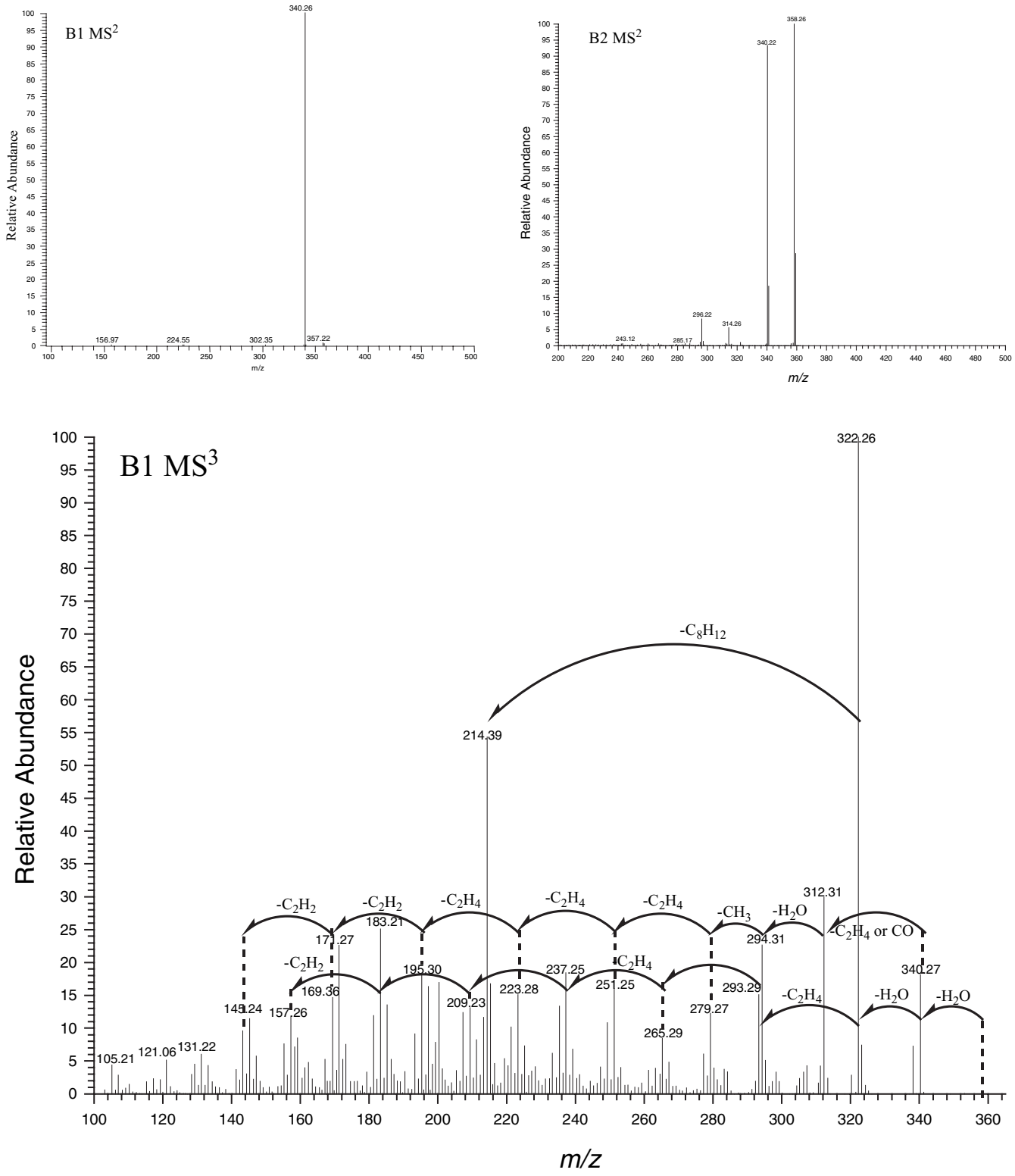

Figure 3. ESI-IT-MS^n mass spectra of isomers B1 and B2. Ions at *m/z* 358 and 340 are the precursor ions in MS^2 and MS^3, respectively.

the ion at *m/z* 314.2462 fragmented to form the ion at *m/z* 296.2357 corresponding to loss of H_2O, while the ion at *m/z* 314.2128 fragmented to produce the ion at *m/z* 300, which can be ascribed to the loss of a methylene from C16 or C4. Fortunately, in subsequent ESI-MS^n experiments of a series of veatchine-type alkaloids with the double bond on the C16 and a methyl on C4, no interval of 14 mass units between two even-mass fragment ions was detected. So, the ion at *m/z* 300 was derived from the loss of the methylene on the C16 and can be viewed as the diagnostic ion.

Apart from the ions discussed above, odd-mass fragment ions with an interval of 14 mass units from *m/z* 253 to 105 were also detected, which cannot be easily explained as tandem loss of CH_2. How to interpret them? One possible answer is

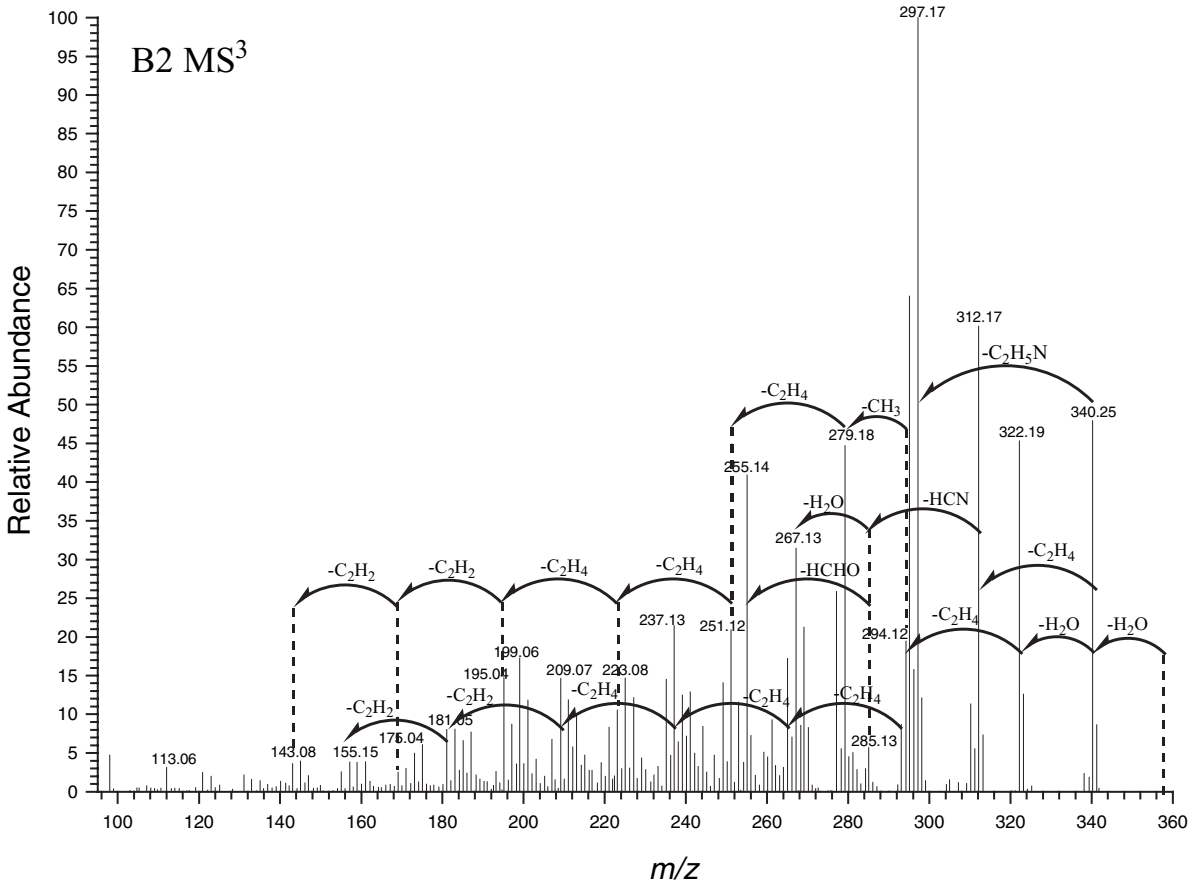

Figure 3. Continued.

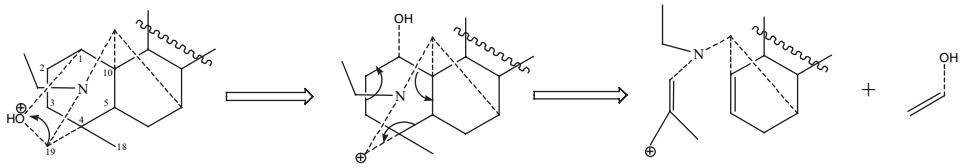

Scheme 4. Proposed fission mechanism of elimination of C_2H_4O in 12-*epi*-dehydronapelline.

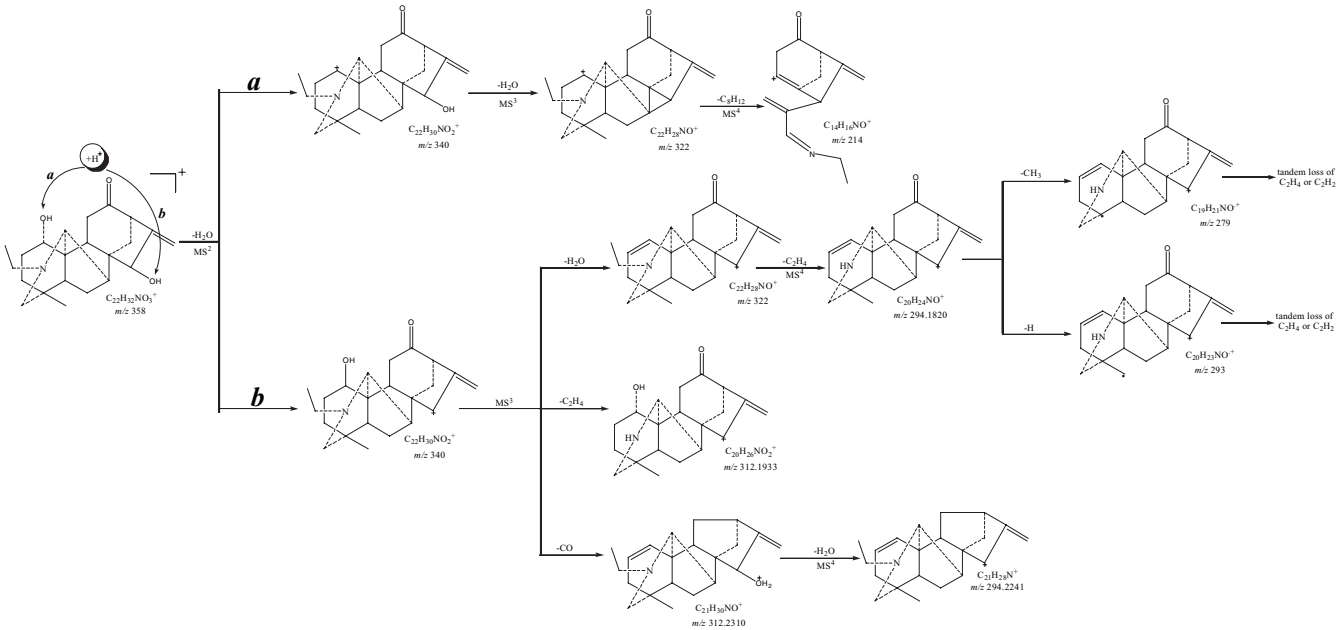

Scheme 5. Proposed fragmentation pathways of songorine from (+)-ESI-IT-MS^n analysis. Accurate mass measurements of ions acquired on ESI-QqTOF-MS/MS are reported in Table 2.

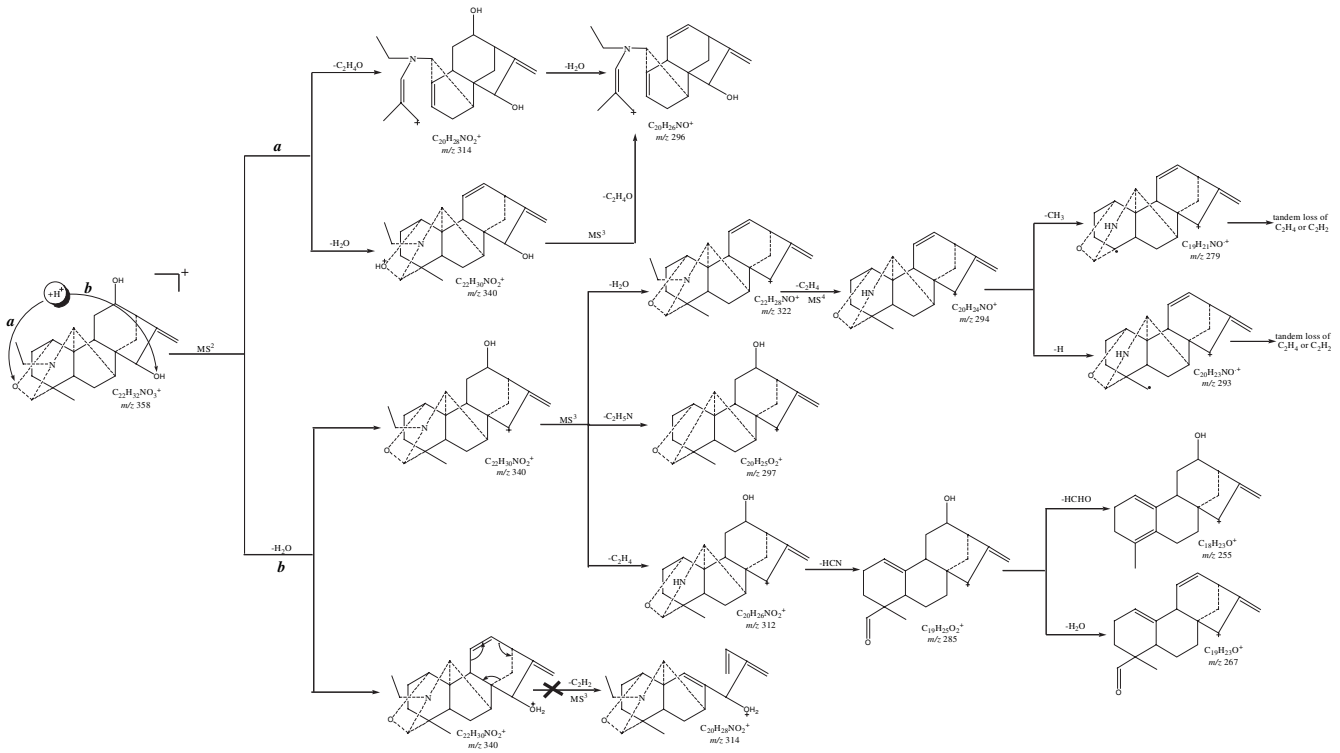

Scheme 6. Proposed fragmentation pathways of 12-*epi*-dehydronapelline from (+)-ESI-IT-MS^n analysis. Accurate mass measurements of ions acquired on ESI-QqTOF-MS/MS are reported in Table 2.

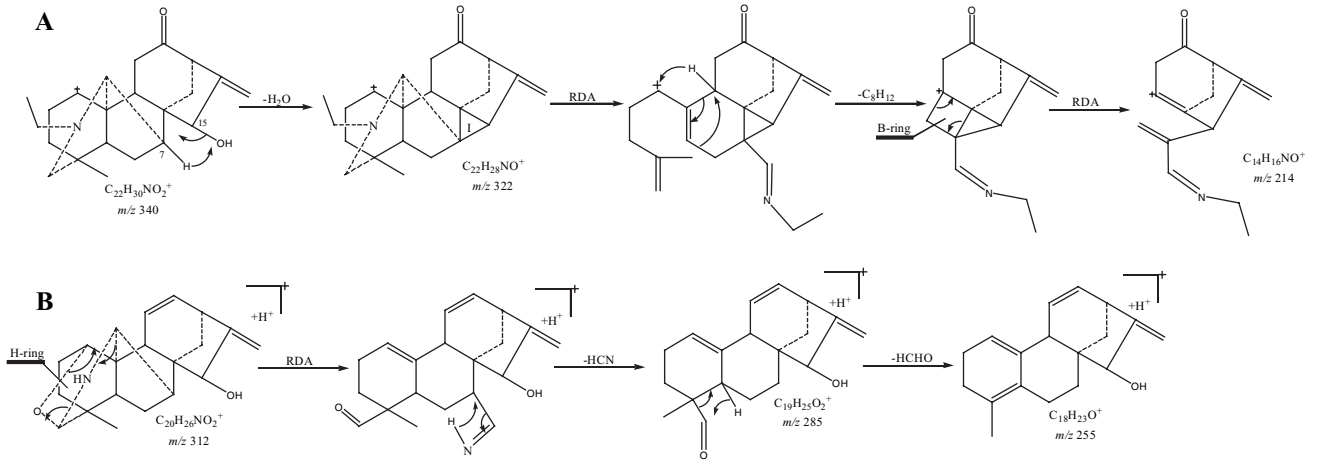

Scheme 7. Mechanisms proposed for fragmentations observed under (+)-ESI-IT-MS^3 analysis: (A) *m/z* 340 → 214 and (B) *m/z* 312 → 285 → 255.

that ions at *m*/*z* 253, 225, 197, 171, 145 and 119 were produced by the tandem loss of three C_2H_4 and three C_2H_2 molecules from the ion at *m*/*z* 281, while the ions at *m*/*z* 267, 239, 211, 183, 157 and 131 can be attributed to the tandem loss of four C_2H_4 and two C_2H_2 molecules from the ion at *m*/*z* 295. The proposed fragmentation processes, which involved a series of single-electron transfers, are depicted in Schemes 2(B) and 2(C).

As far as napelline is concerned, fragment ions in the MS^3 experiment were similar to those of karakomine except for the following ions. First, with three hydroxyls, *m*/*z* 306 was formed by elimination of three H_2O from the precursor ion, while *m*/*z* 263 was produced by the loss of H_2O from the ion at *m*/*z* 281. Second, no ion was detected as loss of CO. Finally, due to the double bond on C16, CH_2 cannot be eliminated to produce the ion at *m*/*z* 300. The proposed fragmentation mechanism is depicted in Scheme 3.

ESI-IT-MS^n and ESI-QqTOF-MS/MS analysis of isomers B1 and B2 (MW 357 Da)

In the positive ion mode using full-scan acquisition, both isomers B1 and B2 yielded protonated molecular ions at *m*/*z* 358, corresponding to songorine[13] or 12-*epi*-dehydronapelline[16] according to the literature. The structural difference between them is that songorine has one carbonyl while 12-*epi*-dehydronapelline has a special oxygen bridge.

Different structures may lead to different fragmentation pathways, so MS/MS experiments were performed to distinguish them. In the MS/MS experiment of isomer B1, only the dehydrated fragment ion at *m/z* 340 was observed, while, in the MS/MS spectra of B2 (Fig. 3), product ions at *m/z* 340, 322, 314 and 296 was observed. Ions at *m/z* 340 and 322 corresponded to loss of one and two H_2O from the precursor ion, respectively. To explain the ion at *m/z* 314, there were two possibilities. One was loss of H_2O and acetylene; the other pathway was that isomer B2 corresponded to 12-*epi*-dehydronapelline and the ion at *m/z* 314 was formed by direct loss of C_2H_4O via the fission of the oxygen bridge and double-electron transfer. Because there was no fragment ion derived from loss of H_2O and acetylene in the MS/MS spectra of karacomine and napeline, the latter pathway is more reasonable. In the MS/MS spectrum of B2, the ratio of relative abundance of ions at *m/z* 340 and 314 is 95 to 6, which confirmed that, although a large portion of protons were added on the hydroxyl group, some protons were adducted to the oxygen bridge, which can further trigger the fission process of the oxygen ring. The bond between C19 and oxygen would be broken and a pair of electrons would be transferred to the oxygen. Then, C19 carried one positive charge, which would lead to the double-electron transfers in C4–C5, C1–C10 and C2–C3 bonds. Thus C_2H_4O was eliminated. The proposed fragmentation mechanism is depicted in Scheme 4. To further validate our assumption, the ion at *m/z* 340 was isolated as the precursor ion in the MS^3 experiment which gave rise to the fragment ions at *m/z* 322$[M+H-2H_2O]^+$, 312$[M+H-H_2O-C_2H_4]^+$ (single peak at *m/z* 312.1974 detected in ESI-QqTOF-MS/MS, indicating that there is no carbonyl in isomer B2), and a series of ions without a signal at *m/z* 314, which further confirmed our assumption that the latter pathway is correct. Therefore, compounds B1 and B2 corresponded to songorine and 12-*epi*-dehydronapelline, respectively. NMR experiments were also performed and the data were in accordance with the literature. Furthermore, the fragmentation pathways of songorine and 12-*epi*-dehydronapelline were proposed by the accurate mass data acquired by ESI-QqTOF-MS/MS (Schemes 5 and 6).

The MS^3 spectrum of songorine is similar to napelline except that some mass data of fragment ions were decreased at 2 Da, e.g. the mass change of ions from *m/z* 216 to 214, 281 to 279 and 267 to 265, indicating that songorine fragmented in a similar fashion to napelline. It should be pointed out that the formation of the ion at *m/z* 214 might not follow the same route as karakomine and napelline. Because there is no hydrogen in the vicinity of C15 in songorine, to retain the positive charge on C1 and lose two H_2O, the proton on C7 would be transferred to the hydroxyl on C15 to eliminate the second H_2O, which gives rise to a new three-membered I-ring. If the C_8H_{12} group was lost, double-electron transfer would occur in the B-ring to lower the instability and high tension produced by the I-ring. The proposed mechanism is depicted in Scheme 7(A). In addition, owing to the presence of a carbonyl group, double peaks at *m/z* 312 and 294 were observed in ESI-QqTOF-MS/MS.

On the other hand, although napelline and 12-*epi*-dehydronapelline are also similar, their fragmentation processes are different, which can be attributed to the oxygen bridge. First, it is notable that the special ion at *m/z* 214 was absent in 12-*epi*-dehydronapelline, which can be explained by the fact that, due to the oxygen bridge, a positive charge could not be formed by the elimination of H_2O from C1, thus there was no incentive to trigger the double-electron transfer and then the C_8H_{12} neutral fragment would not be eliminated. So, the ion at *m/z* 214 is another crucial ion that can be used to distinguish them. Moreover, the ion at *m/z* 285 can be rationalized by the elimination of HCN from the ion at *m/z* 312 through the RDA reaction of the H-ring and double-electron transfer. Then it fragmented further to yield the ions at *m/z* 267 and 255, corresponding to loss of H_2O and HCHO, respectively. Proposed fragmentation mechanisms are depicted in Scheme 7(B).

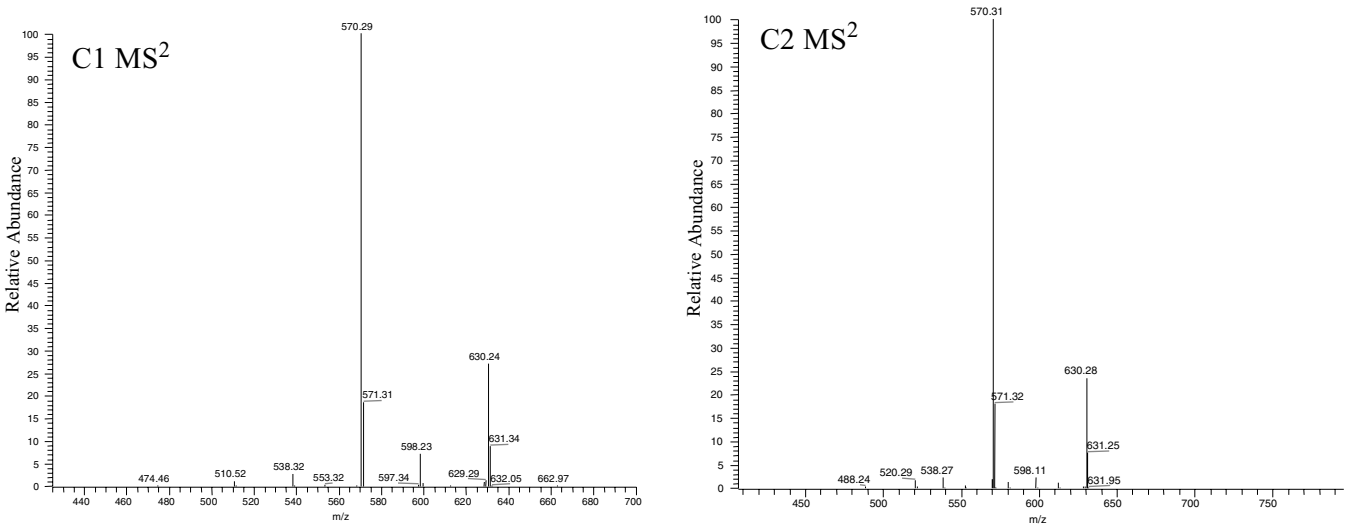

Figure 4. ESI-IT-MS^n mass spectra of isomers C1 and C2. Ions at *m/z* 630 and 570 are the precursor ions in MS^2 and MS^3, respectively.

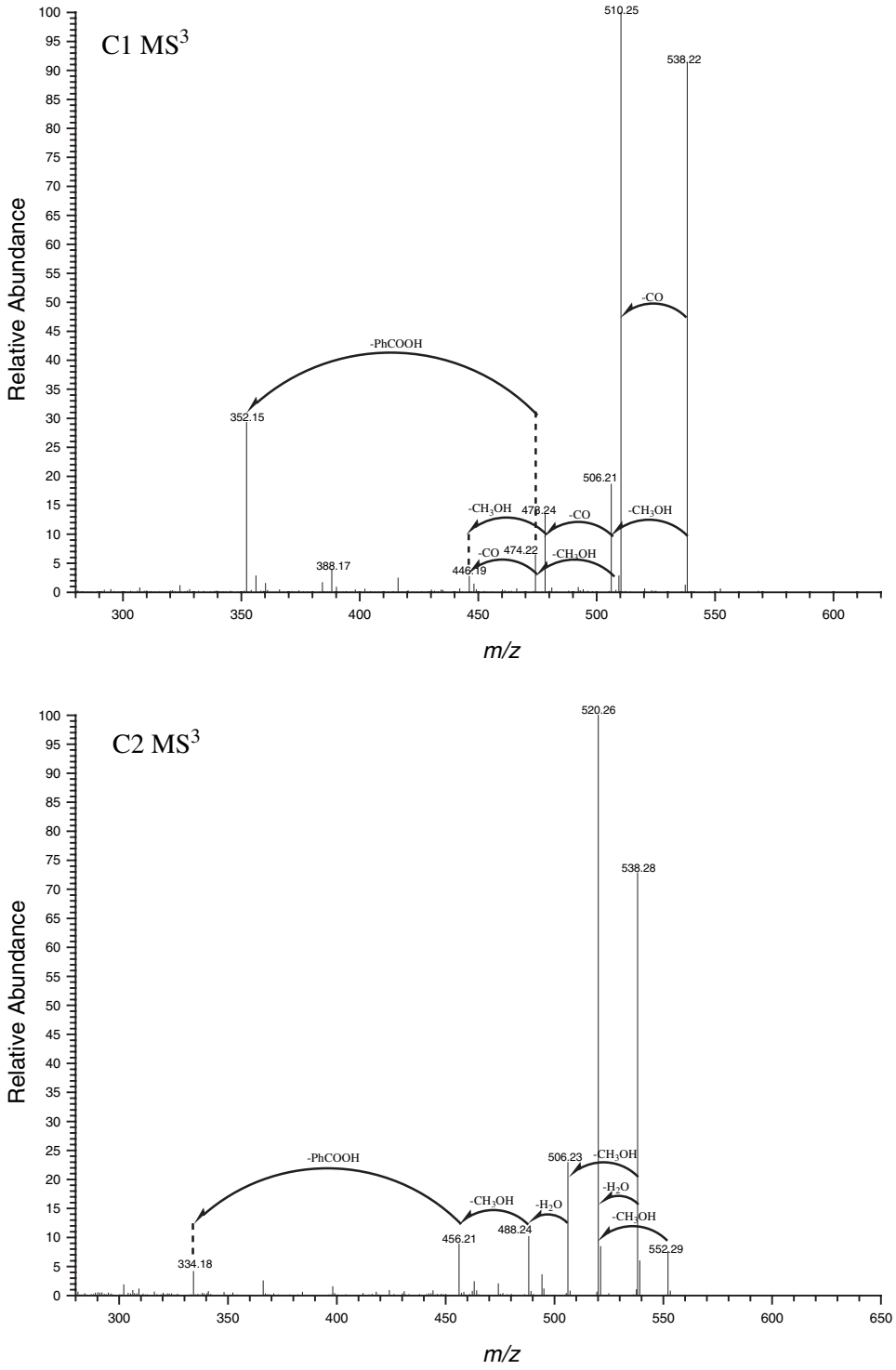

Figure 4. Continued.

Fragmentation laws of some veatchine-type alkaloids in positive ESI mode

Through analysis of the above four veatchine-type alkaloids by ESI-MS/MS, the fragmentation laws were concluded. First, the principal fission pathway is loss of peripheral hydroxyl, carbonyl and the N-substituent, in which all the fragment ions are even and usually detected in high abundance. Second, the CH_3 radical or hydrogen would be readily eliminated via the homolysis of C18–C4 or C18–H bonds to form the ions with odd mass, followed by elimination of a series of C_2H_4 and C_2H_2. Third, the RDA reaction occurs in the E-ring and double-electron transfer triggered by the positive charge on C1 will lead to the formation of diagnostic ions at *m/z* 214 or 216.

ESI-IT-MS^n and ESI-QqTOF-MS/MS analysis of isomers C1 and C2 (MW 629 Da)

In the first-order ESI mass spectra, both compounds C1 and C2 yielded a protonated molecule $[M+H]^+$ at *m/z* 630 in positive mode, which suggested a molecular mass of 629 Da. However, indaconitine[15] and deoxyaconitine[13] are isomers in which the structural difference resides only in the position

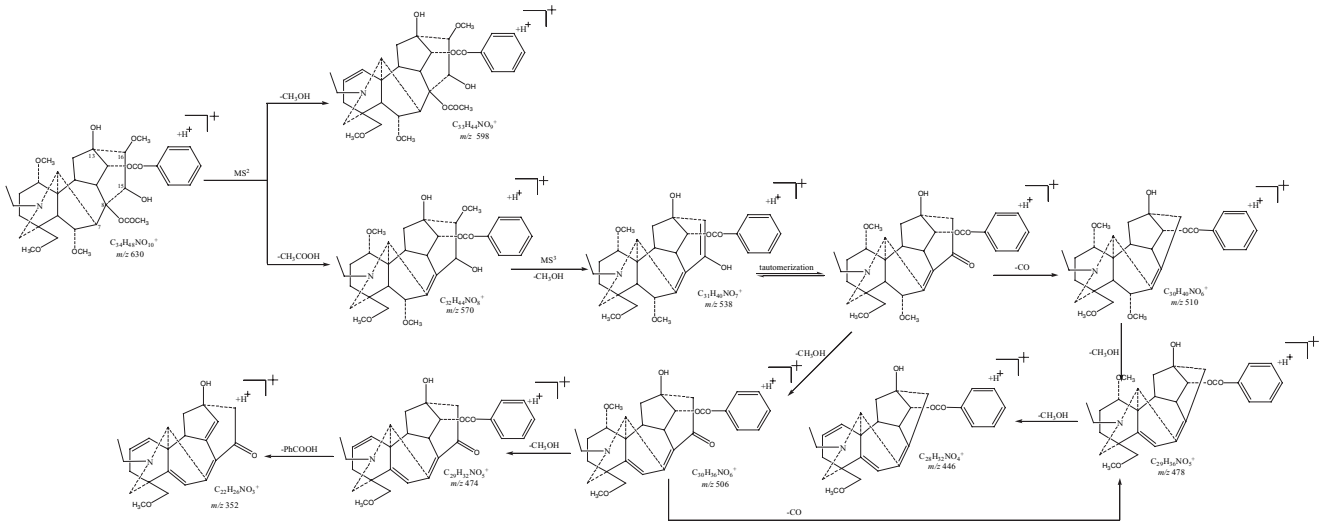

Scheme 8. Proposed fragmentation pathways of deoxyaconitine from (+)-ESI-IT-MS^n analysis. Accurate mass measurements of ions acquired on ESI-QqTOF-MS/MS were reported in Table 2.

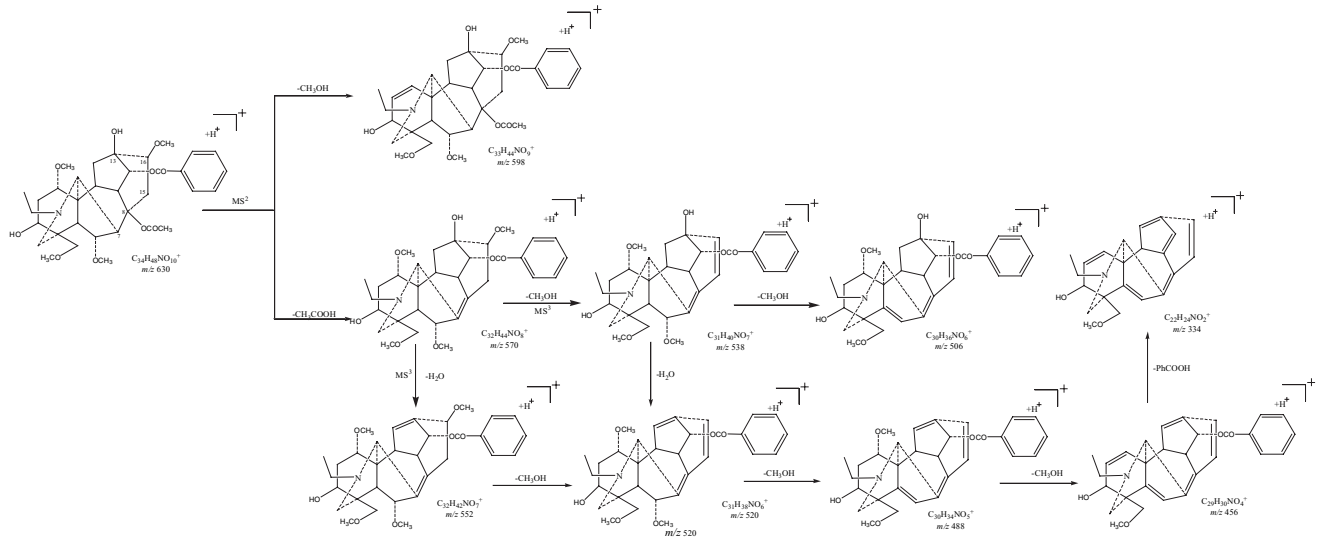

Scheme 9. Proposed fragmentation pathways of indaconitine from (+)-ESI-IT-MS^n analysis. Accurate mass measurements of ions acquired on ESI-QqTOF-MS/MS are reported in Table 2.

of the hydroxyl group. To differentiate them, ESI-IT-MS^n experiments were carried out. In ESI-MS/MS of C1 and C2 (Fig. 4), the predominant ion appeared at *m/z* 570 corresponding to the elimination of HAc (acetic acid) from C8. Ions at *m/z* 598 and 538 were also detected in low abundance corresponding to the loss of a methoxyl group and combined loss of acetic acid and methoxyl, respectively. In the ESI-MS^3 experiment with the precursor ion at *m/z* 570 (collision energy: 30%), the product ions of isomer C1 included *m/z* 538, 510, 506, 478, 474 and 352, while the ions at *m/z* 552, 538, 520, 506, 488, 456 and 334 were detected in isomer C2. Among them, ions at *m/z* 552, 538, 520, 506, 488, 474, 456, 352 and 334 can be easily interpreted by losses of water, methanol, benzoic acid or a combination of these. How to interpret the ions at *m/z* 510 and 478 in isomer C1? One possibility was that isomer C1 corresponded to deoxyaconitine, in which there is a hydroxyl on C15 and a methoxyl on C16. When the methoxyl on C16 was eliminated together with the vicinal proton on C15 as a methanol, the double bond was formed and enol was produced. Then, the enol tautomerized into carbonyl and CO was lost. In the process of loss of CO, it is the methoxyl of C16, hydroxyl of C15 and hydrogen of C15 that played the key role. (In the following work, we worked on a series of aconitine-type alkaloids possessing the similar structure and found the same law that can be applied in detecting whether there are hydroxyl and methoxyl on the C15 and C16, respectively.) On the other hand, although there is a hydroxyl on C13 and a methoxyl on C16 in indaconitine, an enol could not be formed due to loss of hydrogen in C13. Since there was no ion corresponding to loss of CO in isomer C2, it should be indaconitine. HR-ESI-MS/MS and NMR experiments were also performed and data were consistent with the literature. Proposed fragmentation mechanisms of deoxyaconitine and indaconitine are depicted in Schemes 8 and 9.

Difference of fission law of veatchine and aconitine alkaloids in ESI-MS^n mode

Among the three pairs of isomers, compounds A1, A2, B1 and B2 are veatchine-type alkaloids; compounds C1 and C2 are aconitine-type alkaloids. From the above MS/MS analysis together with research of aconitine-type alkaloids,[11,12] comparisons of fragmentation pathways of veatchines and aconitines were conducted. They share the common principal fission pattern as tandem loss of peripheral moieties as 1–3 H_2O or 1–4 CH_3OH. But they are different in many aspects. To acquire the crucial fragment ions, veatchines need more collision energy (with a collision of 40%). The fragment ions of aconitine-type alkaloids are neat and have relative high abundance, whereas the fragment ions of veatchine-type alkaloids are cluttered and have weak intensity. The most important differences reside in the following three facets. First, in veatchine-type alkaloids, radicals would be readily formed by the homolysis of C18–C4 or C18–H bonds followed by the tandem loss of C_2H_4 and C_2H_2, which leads to the formation of fragment ions with odd mass. However, in aconitine-type alkaloids, almost all the fragment ions bear the even mass. Secondly, although there is no carbonyl in some aconitine-type alkaloids, with the hydroxyl and methyl on C15 and C16, respectively, CO can be eliminated through tautomerization. Finally, as for veatchine-type alkaloids, ethylene would be readily eliminated from nitrogen; however, in aconitine-type alkaloids, to lose an ethylene is not as favorable.

CONCLUSIONS

ESI-IT-MS^n and ESI-QqTOF combined with tandem mass spectrometry (MS/MS) has been proved to be a fast and effective method for analysis of aconite alkaloids. Accurate mass measurements of product ions allowed ambiguities to be removed concerning neutral losses having the same nominal mass, CO and C_2H_4, allowing the fragmentation patterns to be rationalized. The fragmentation pathways of veatchine- and aconitine-type alkaloids are different, by which veatchine- and aconitine-type alkaloids can be easily differentiated. Furthermore, some isomers of aconite alkaloids can be differentiated.

REFERENCES

1. Dong JY, Li L. *J. Plant Resour. Environ*. 2000; **9**: 1.
2. Chen SY, Li SH, Hao XJ. *Acta Bot. Sinica* 1986; **28**: 86.
3. Zhang SX, Jia SS. *Acta Pharm. Sincia* (in Chinese) 1999; **34**: 762.
4. Sayed HM, Desai HK, Ross SA, Pelletier SW. *J. Nat. Prod*. 1992; **55**: 1595.
5. Shrestha PM, Katz A. *J. Nat. Prod*. 2000; **63**: 2.
6. Wang FP, Li ZB, Wang JZ. *Acta Chim. Sinica* (in Chinese) 2000; **58**: 576.
7. Wada K, Bando H, Kawahara N. *J. Chromatogr*. 1993; **644**: 43.
8. Ito K, Ohyama Y, Hishinuma T, Mizugaki M. *Planta Med*. 1996; **62**: 57.
9. Ohta H, Seto Y, Tsunoda N. *J. Chromatogr. B* 1997; **691**: 351.
10. Wada K, Mori T, Kawahara N. *J. Mass Spectrom*. 2000; **35**: 432.
11. Wang Y, Liu ZQ, Song FR, Liu SY. *Rapid Commun. Mass Spectrom*. 2002; **16**: 2075.
12. Wang Y, Song FR, Xu QX, Liu ZQ, Liu SY. *J. Mass Spectrom*. 2003; **38**: 962.
13. Ding LS, Wu FE, Chen YZ. *Nat. Prod. R&D* 1994; **6**: 50.
14. Zhen PJ, Wang M, Wang BY, Tian RM, Jiang SH, Zhou BN. *Acta Chim. Sinica* 1987; **45**: 328.
15. Pelletier SW, Mody NV, Sawhney RS, Bhattacharyya J. *Heterocycles* 1977; **7**: 327.
16. Rahman AU. *Handbook of Natural Products Data*, vol. 1, *Diterpenoid and Steroidal Alkaloids*. Elsevier: New York, 1990; 321.